

14<sup>th</sup> Congress of the International Society for Photogrammetry

Hamburg 1980

Commission I

W.G. 1 / 2 Image Geometry with Camera Calibration

Presented Paper

J.Hakkarainen

Finnish Geodetic Institute, Helsinki

K.-J.Rosenbruch

PTB, Braunschweig

Studies on Image Evaluation Methods and Lens Aberrations

Abstract

The first-mentioned author was with Alexander von Humboldt-fellowship in the PTB in Braunschweig in 1978-79. The author had an aerial wide-angle lens Wild RC-8 15Ag from Finland with him for measurements. The focal length, spherical aberration, coma, field curvature, astigmatism, influence of defocusing on the axis, point images, and MTF for seven field angles were determined from this lens in the PTB. The geometrical errors, resolving power and MTF were determined from the same lens with the Helsinki University of Technology (HUT) goniometer. MTF values in Braunschweig and Helsinki were the same with an adequate accuracy. The method used in Helsinki gives on an average from 3 to 10 % greater values than the EROS method used in the PTB depending somewhat on the field angle.

## Introduction

The lens quality can mainly be described with lens aberrations, resolving power or MTF, or also with a criteria connected with the discerning of some image details. In this study the relation between the resolving power and MTF, and the lens aberrations is dealt with. A comparison between two different MTF determination methods has also been made.

The first-mentioned author was with the Alexander von Humboldt-fellowship in the Department of optics of the PTB in Braunschweig in 1978-79 having an aerial wide-angle lens RC-8 15Ag No.102 from Finland with him for measurements. For studying the above-mentioned subject the focal length, spherical aberration, coma, field curvature and astigmatism, point images and the influence of defocusing on the RP on axis were determined in the PTB in winter 1979. Also MTF measurements for 7 field angles were accomplished. The lens cone was detached from the camera body for measurements in the PTB. Additionally the geometrical calibration of the camera was made by Wild Heerbrugg on May. The aim was to clear up whether the detaching of the lens from the camera body had had any influence on the image geometry. In the summer 1979 the first-mentioned author finally made a complete calibration and MTF measurement for the camera with the goniometer in Helsinki. Because all these measuring methods are well-known, the interest is directed mainly on the results in this paper.

### 1 Focal length and aberrations

#### 1.1 Focal length

The focal length was measured with an equipment constructed in the PTB for the measurement of lenses with a long focal length. The measuring principle is as follows:

$$f = \frac{y'}{\tan \omega} \quad \omega \text{ is a small angle ( see fig. 1.)}$$

The determination was made with  $y'$  values of 4, 5, 6 and 8 mm. The angles  $\omega$  were measured with a theodolite. The result was that the effective focal length of the 15Ag No.102 lens was 153.36 mm. The calibrated focal length determined in Helsinki was 153.35 mm and that by Wild 153.34 mm.

#### 1.2 Spherical aberration and coma

The spherical aberration and the coma were determined with the Hartmann method /1/. A parallel bundle of rays coming from a two-meters-collimator was exposed on intra-and extrafocal photo plates. The star images formed on these were measured with an Abbe-comparator. The aberrations were calculated as intersections of the straight lines between intra-and extrafocal points. Because the aerial lens could not be turned in the optical bench due to its big size, its centering was not good enough. As a consequence the points near the optical axis remain very uncertain. The results are shown in the figures 2 and 3.

### 1.3 Field curvature and astigmatism

The sagittal and tangential field curvatures were determined in the Wett-hauer bench by measuring the places of the best focus with a microscope in 19 field angles from  $0^{\circ}$  to  $45^{\circ}$ . In the fig. 4. we can see that the field curvatures are rather symmetrical in the direction A-C. The astigmatism is very great when the field angle is greater than  $38^{\circ}$  ( $r > 120$  mm) and great when  $r = 40 - 90$  mm.

### 1.4 Distortion

The radial and tangential distortions were measured in Helsinki with the goniometer. The results are in the figures 5 and 6. The camera has a very good symmetry in the direction B-D. The asymmetry in the diagonal A-C is caused by the decentering of one or more lens elements in this direction. The axis of the maximal asymmetry of radial distortion and the 0-axis of the tangential distortion are about the same. The ratio between the radial and tangential components of the decentering is 3. The determination of the radial distortion in the corner of the image with the HUT goniometer is uncertain because of the phase shift phenomenon. Therefore the radial distortion has been notified only up to the value of  $r = 100$  mm. Up to this value the place of the grid cross in an inclined position could be determined without difficulties.

### 1.5 Lateral chromatic aberration

Lateral chromatic aberration was measured with the goniometer in the spectral region from 450 nm to 650 nm. A continuous monochromatic filter was behind the eyepiece of the observing telescope. The results are in the fig. 7.

### 1.6 Point images

The images of a bright point were observed and drawn in the Wett-hauer bench using a microscope. The size of the point was 0.08 mm in the middle point of the image. The observations were made in the plane of best definition determined on the optical axis and with defocusing of  $\pm 0.5$  mm and  $\pm 1.0$  mm in field angles from  $0^{\circ}$  to  $45^{\circ}$ . The results drawn are in the fig. 8. In some cases it is difficult to determine the weight point of the image of the bright point even in the plane of best definition.

## 2 Resolution

### 2.1 Resolving power in goniometer

The optical resolving power of the camera was determined with the goniometer using a test plate on the frame plane. There were 9 groups of test figures in the plate in one radius. The greatest spatial frequency was 220 L/mm. The contrast at the order of 100 L/mm is 1.6 and at the order of 200 L/mm 1.0. The RP values are given in the fig. 9. The figures can be photographed through the lens and observing telescope. When the figures 4. and 9. are compared, there can be seen clearly that the field curvature of 0.15 mm has a strong decreasing influence on the RP.

The dependence of the radial RP on the aperture with the values 1:5.6,8,11 and 16 is shown in the fig. 10. The determination was made visually. The trend of tangential lines is about the same.

## 2.2 Resolving power on axis determined in the Wetthauer bench

The influence of the aperture and the relation between the RP and the diffraction limit are shown in the fig. 11.

## 2.3 Influence of defocusing on the RP on axis

The influence of the defocusing on axis is presented in the fig. 12. The observations were made in the Wetthauer bench with square wave high contrast test targets. The maximum RP with the aperture of 5.6 was about 270 L/mm. Phase shift of  $180^\circ$  or spurious resolution occurs both inside and outside the best focus. About 0.3 mm outside the best focus there is also a region of normal image formation, but with a weak modulation.

## 3 MTF measurements

### 3.1 MTF methods

Nowadays many MTF methods with different principles are used. When comparing the MTF values of the same lens measured in different laboratories it has been verified that the agreement of the results on axis is good, but outside the axis, especially with great field angles, large differences may be found.

#### 3.1.1 Method in the PTB

In the PTB the EROS method is used. The test target is in principle a parallelogram. The lens to be studied is stationary on the optical bench. The transmitter is on a carriage on an optical bench which is perpendicular to the primary bench at a distance of 6 m from the lens. The receiver is moving on the horizontal diameter in the image plane respectively. So it is possible to measure the MTF's of field angles up to  $45^\circ$  outside the axis. The output signal is measured with a slit. The right receiver field angle is adjusted with the phase of a gross spatial frequency. The EROS method gives both the MTF and the phase transfer. Plus-minus 4 % is given for the precision of the method. The difference between  $\infty$  and 6 m causes an error of about 1 % on the MTF.

#### 3.1.2 Method in Helsinki

In the method used in Helsinki the test target is on the frame plane of the camera to be studied (see section 2.1). The figures are photographed through the observing telescope with an enlargement of about 10x on the film of the register camera. The MTF is calculated from the measurements made from this film. The main steps of the method are:

- 1) Goniometer photography.
- 2) Microdensitometer measurements.

- 3) Sensitometric exposure of the register film.
- 4) Microdensitometer values to effective exposure values with the characteristic curve.
- 5) Calculation of the square wave modulation.
- 6) Square wave modulation to the MTF with Fourier analysis.
- 7) Corrections caused by the microdensitometer slit and object figures.
- 8) MTF of the register film and the adjacency effect influence in the opposite directions. The errors caused by them and the goniometer optics remain as error factors of the method.

### 3.2 Reference plane

The place of the plane of best definition was determined in the Wetthauer bench with the wave length of 548 nm. Its distance from the last lens surface was 58.44 mm. The corresponding distance of the frame plane measured mechanically was 0.05 mm longer.

When the plane of best definition was measured with 6 different wave lengths the difference between the distances measured with the filters of 548 nm and 585 nm was 0.06 mm. This means that the plane of best definition was in Helsinki very near the frame plane with this illumination. In order to have the reference planes in Braunschweig and Helsinki as close to each other as possible, the 585 nm filter was chosen for the MTF measurements in the PTB, because the spectral weight point in Helsinki was 580 nm.

### 3.3 Comparison between the PTB and Helsinki methods

MTF for the radius A of the RC-8 15Ag No.102 camera was measured in the same 7 field angles in Braunschweig and Helsinki. The results are in the figures 14. We can see that in general the measurement in Helsinki has given about from 3 to 10 % greater values than the measurement in Braunschweig. The differences in % are in the table 1. The differences are largest at spatial frequencies from 10 to 30 L/mm when the field angle is 27.5°, 33.1° and 37.6°. It can be concluded from the results that the accuracy of the method developed in Helsinki is satisfactory. The method is suitable for the comparison measurements of different cameras.

### 3.4 Symmetry of the MTF

The distortion measurements show that the lens elements have moved in the direction A-C. The MTF measurement in the PTB gave some % better values for the radial lines in the direction A and for tangential lines in the direction B. The symmetry was studied in Helsinki by measuring the MTF for all four radii A, B, C and D in the field angles of 27.5° and 37.6°. Differences between different radii were small (See figures 15. and 16.).

### 3.5 Influence of different factors on the MTF

#### 3.5.1 Defocusing

The MTF was measured in the PTB with the defocusing of  $\pm 0.05$  and  $\pm 0.10$  mm for all 7 field angles. The results of angles 0°, 27.5° and 37.6° are in the figures 17, 18 and 19. Because of different field curvatures the effect of the defocusing is changing much. The influence of the field curvature

appears as differences between the MTF's of the plane of best definition and MTF of the reference plane.

### 3.5.2 Wave length of light

The MTF curves of 6 different wave lengths in the plane of best definition are in the fig. 20. We see that the MTF of the blue is remarkably worse than that of the other colors.

### 3.5.3 MTF's on the plane of best definition in different field angles

The results for the different field angles with the light of 585 nm on the plane of best definition are in the figures 21. The difference between the MTF of a diffraction limited system and axis of the 15Ag No.102 expresses the influence of the spherical aberration. The differences between the MTF's on axis and in different field angles are caused mainly by the coma. The influence of the coma is much greater on the tangential MTF than the radial MTF.

## 4 Phase shift phenomenon

The phase shift phenomenon appears in the 15Ag No.102 lens both in radial and tangential lines. The phenomenon arises when the field curvature is great enough. When the curvature is outwards, as with the values of  $r = 40 - 80$  mm ( $14.6^\circ - 27.5^\circ$ ) in the sagittal lines, the figures become grey after the RP limit. When the curvature is inwards a strong phase shift which develops a spurious resolution is in the corner of the image. The outwards-directed field curvature by tangential lines results in a rather strong one-sided image. The harmonics with different spatial frequencies move clearly by different amounts of defocusing from the original place.

The fig. 12. shows that the spurious resolution can be generated in both intrafocal and extrafocal region, in the extrafocal region by very high frequencies. A rather strong region of normal image formation has been generated in a wide spatial frequency region with a defocusing of 0.3 mm outwards in the case of this camera. It was verified with the MTF measurement that the modulation value there was 12 %. The pseudo-MTF inside the focus was 16 % in the maximum. The visual observation showed that the spurious resolution is generated by a very little amount of defocusing after the grey region, which is between the normal and spurious resolution. The phase shift causes also zones of illegal image formation. The above-mentioned pseudo-phenomena occur only rarely in the aerial negative. Instead they are a remarkable drawback in the geometrical laboratory calibration.

## 5 Stability of the 15Ag No.102 lens

First the lens was kept one month on the optical bench in the horizontal position so that the diagonal A-C was horizontally. After this it was turned  $180^\circ$ . In this position it remained 2 months, after which it was removed onto another optical bench where it stayed 1.5 months in the same position. One half year thereafter it was measured in Helsinki. In the measurement it was verified that the decentering component of the radial distortion and the

tangential distortion were the same as earlier with an accuracy of  $\pm 1 \mu\text{m}$ . The calibrated focal length had changed only  $6 \mu\text{m}$  because of the dismantling of the camera in the PTB. So the stability of the 15Ag No.102 lens seems to be excellent.

#### Conclusion

The field curvature mainly gives the form for the RP curve. Some tenth parts of mm of field curvature are needed to generate the spurious resolution. It can be inside or outside the focus. The MTF method developed in Helsinki seems to be accurate enough for comparison measurements of cameras. The RC-8 15Ag camera can also be kept in the horizontal position for long times without a danger that the lens elements move.

#### References :

- Flügge, J.: Das photographische Objektiv  
Wien 1955
- Hakkarainen, J.: Image Evaluation of Reseau Cameras  
Photogrammetria, 33 (1977) pp.115-132
- Rosenbruch, K.-J.: Considerations Regarding Image Geometry and Quality  
Photogrammetria, 33 (1977) pp.155-169

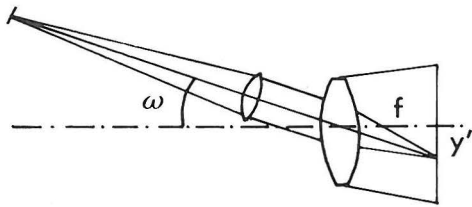


Fig. 1. Measurement of the focal length.

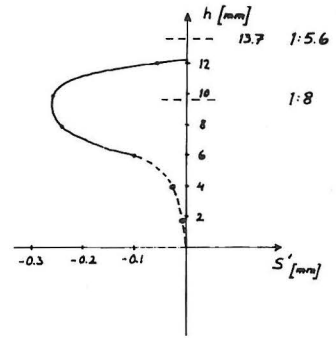


Fig. 2. Spherical aberration.

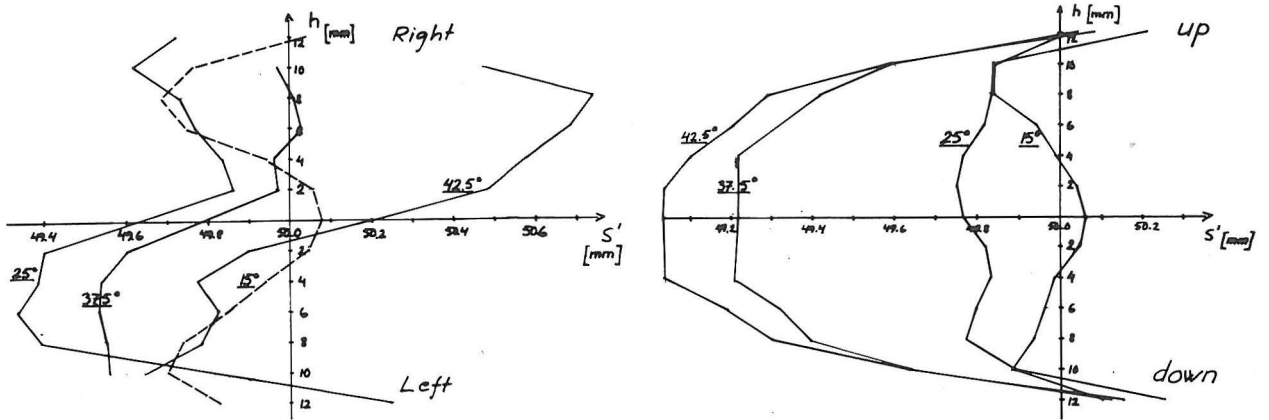


Fig. 3. Coma and spherical aberration at field angles  $15^\circ$ ,  $25^\circ$ ,  $37.5^\circ$  and  $42.5^\circ$ .

a) Right - Left

b) Up - Down

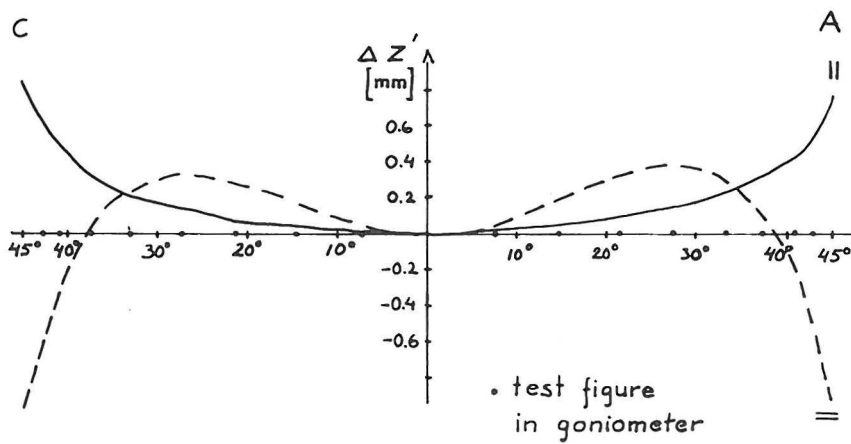


Fig. 4. Field curvature.



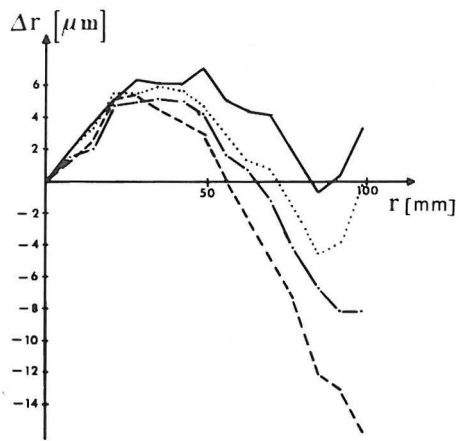


Fig. 5. Radial distortion, origin at PPA.

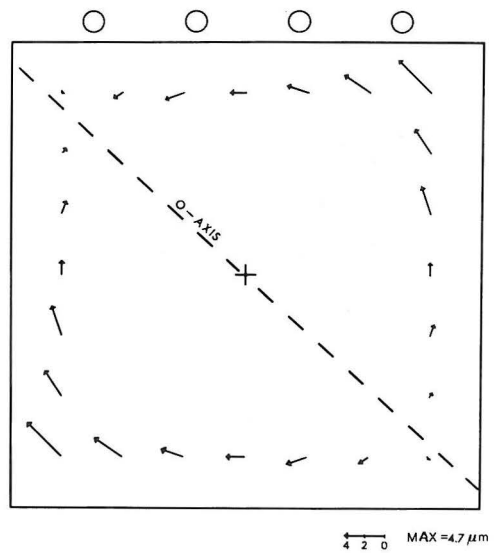
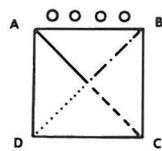


Fig. 6. Tangential distortion.

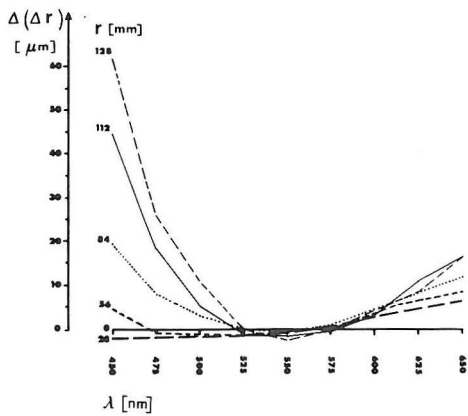


Fig. 7. Lateral chromatic aberration.

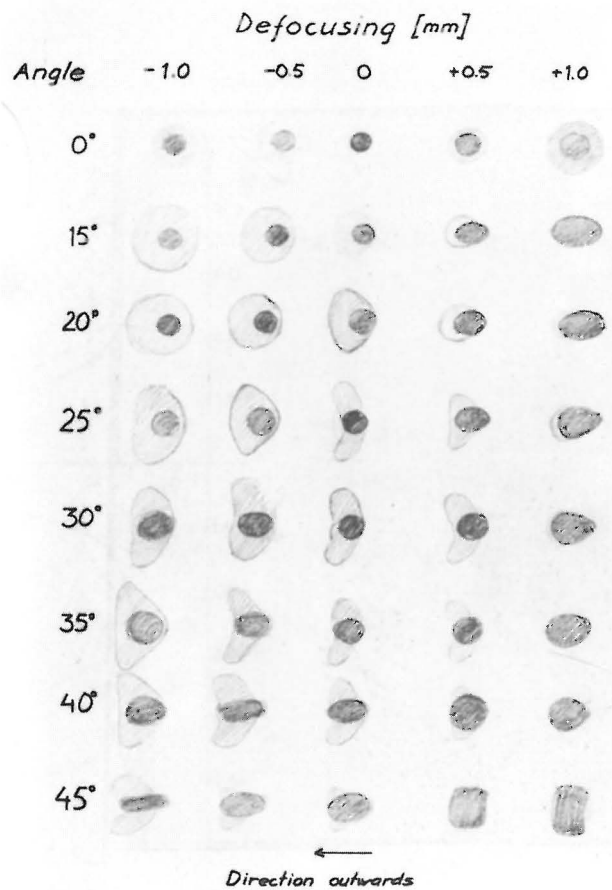


Fig. 8. Images of a bright point, size 0.08 mm on the axis.

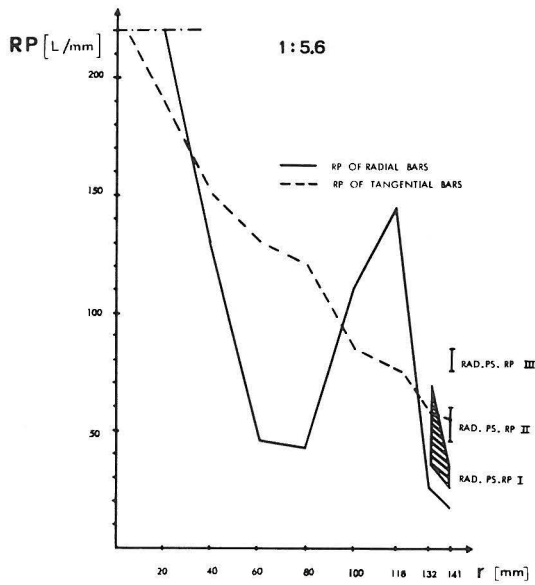


Fig. 9. Resolving power.

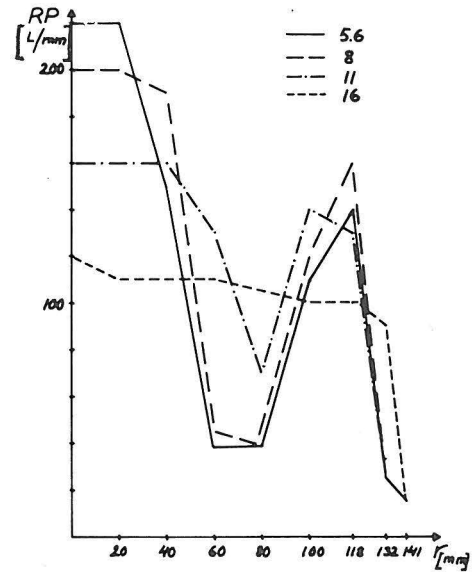


Fig. 10. Radial RP with apertures 5.6, 8, 11 and 16.

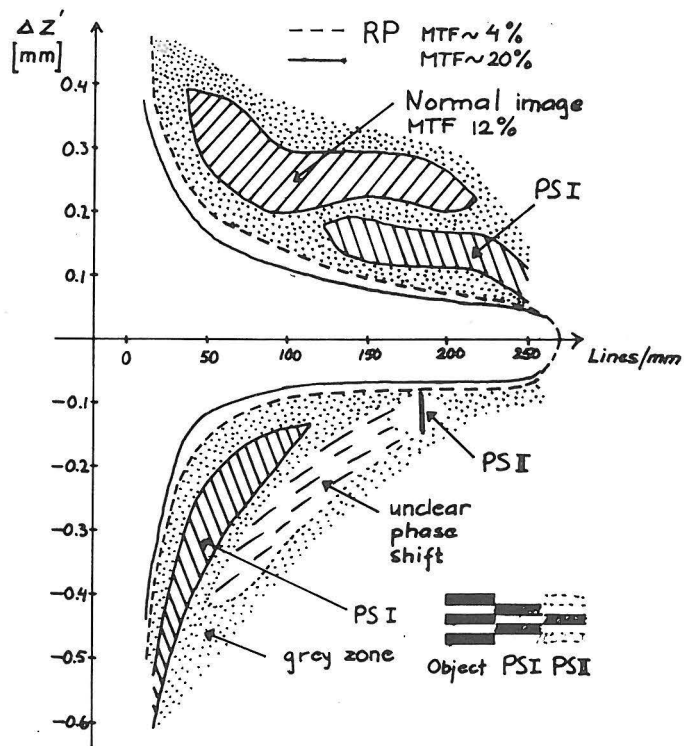


Fig. 12. Influence of defocusing on the axis.

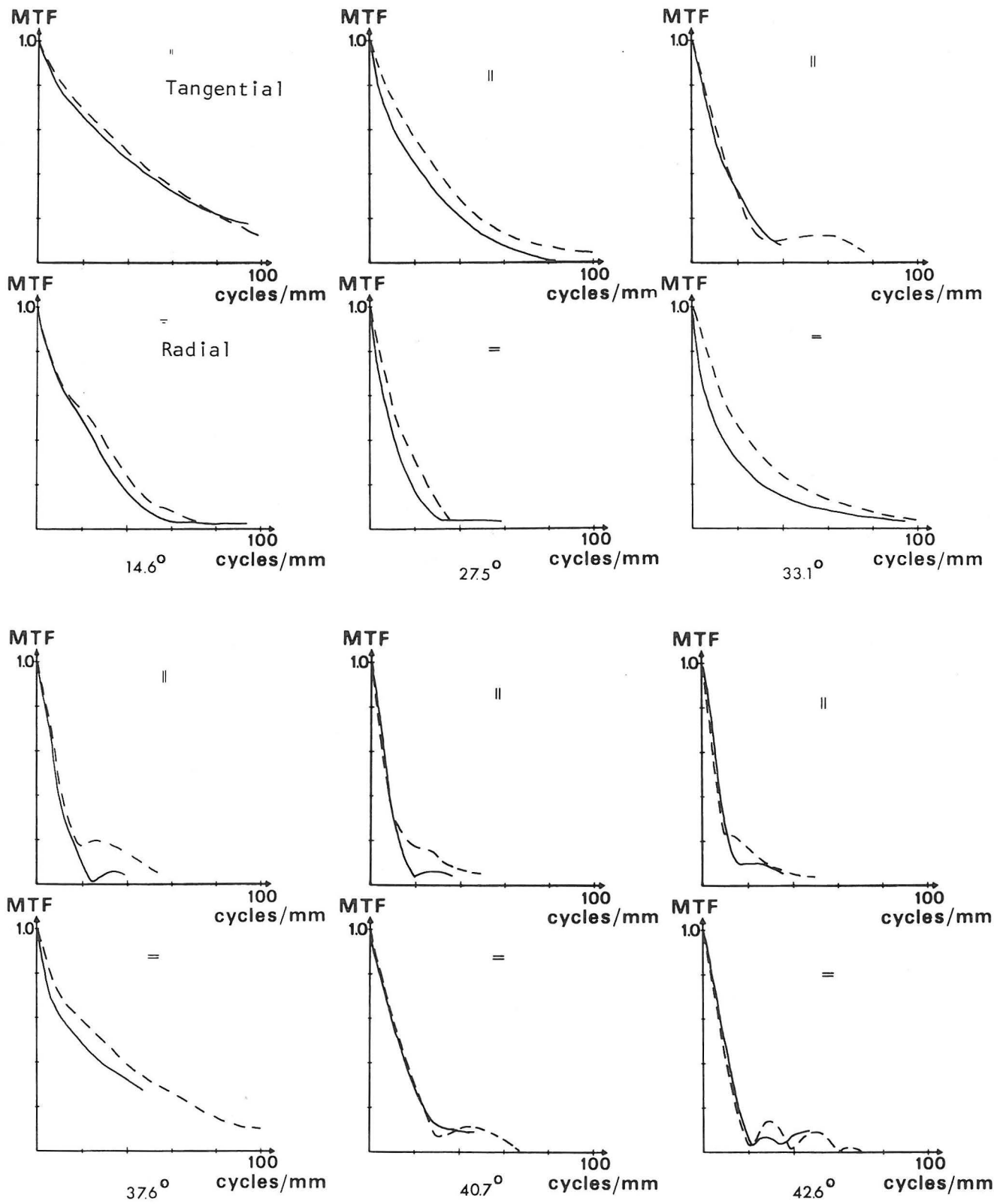


Fig. 14. Comparison between the MTF values achieved in Braunschweig and Helsinki

— Braunschweig      - - - Helsinki

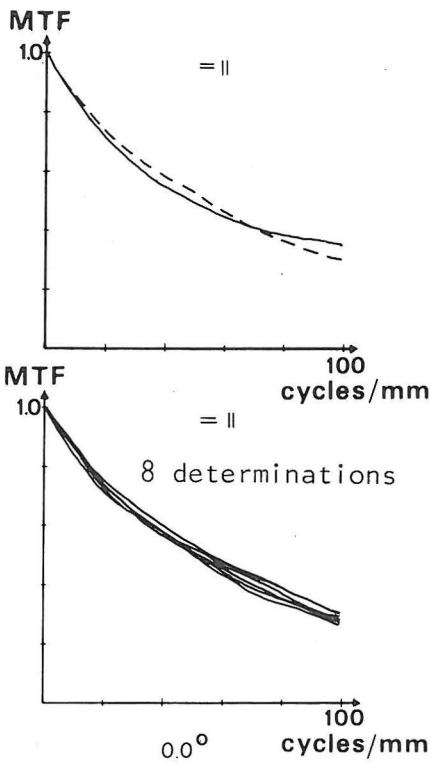


Fig. 14. (continued).

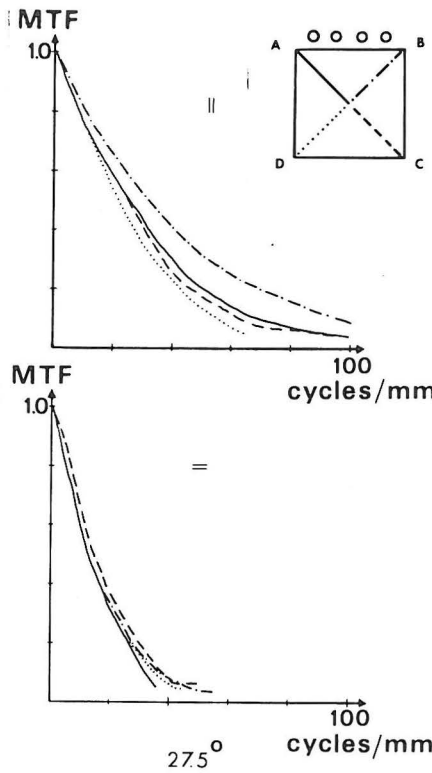


Fig. 15. Symmetry.

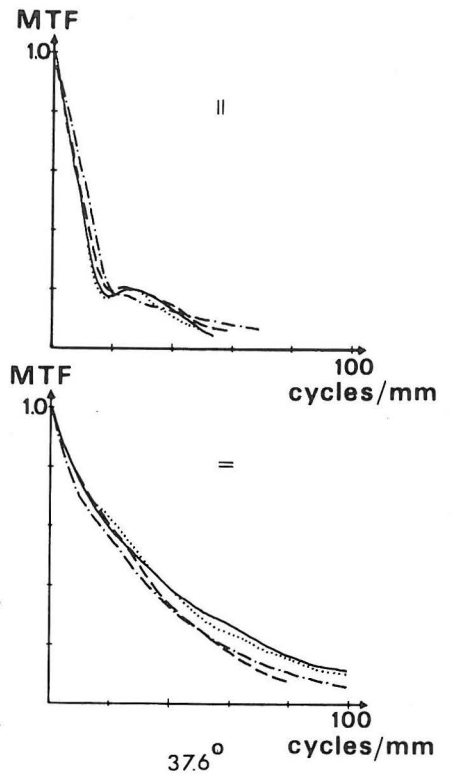


Fig. 16. Symmetry.

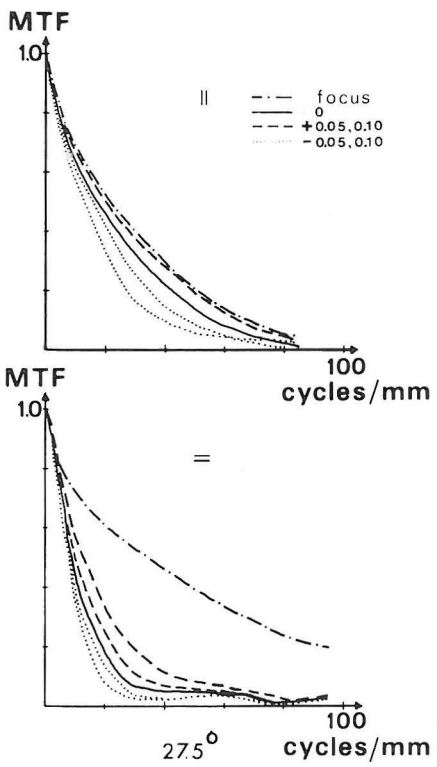


Fig. 17. Effect of defocusing.

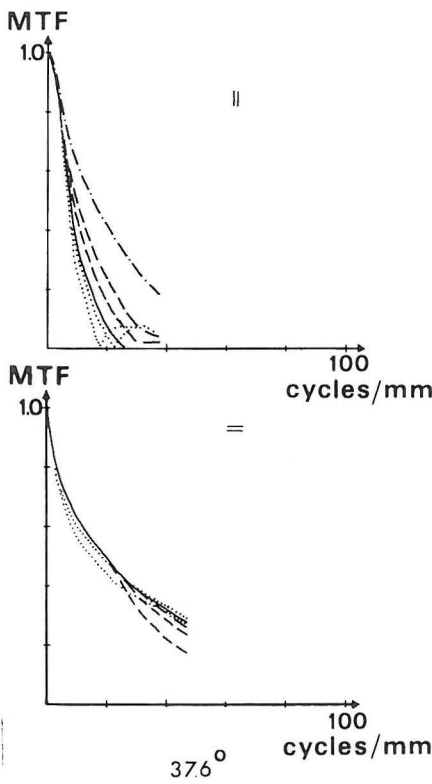


Fig. 18. Effect of defocusing.

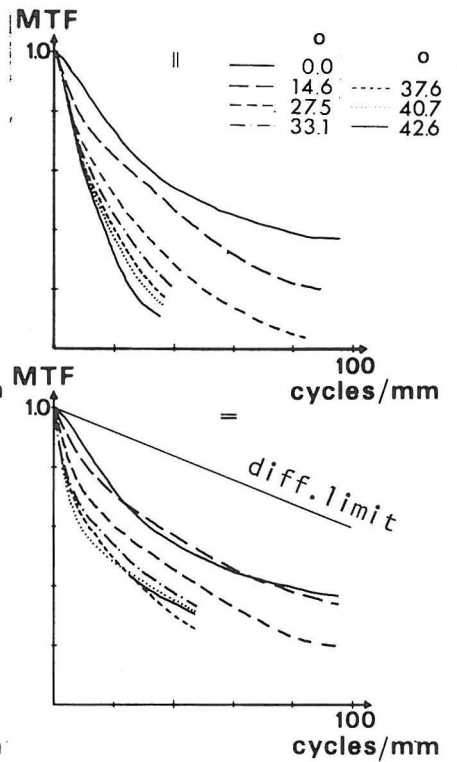


Fig. 21. MTF's of different field angles on the plane of best definition.

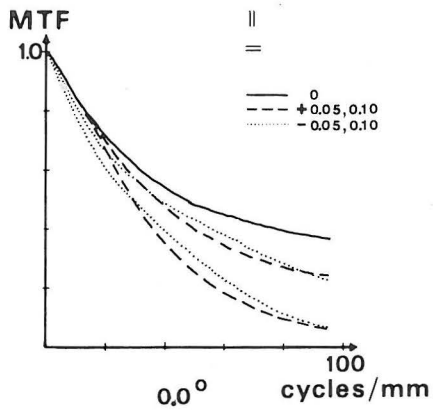


Fig. 19. Effect of defocusing.

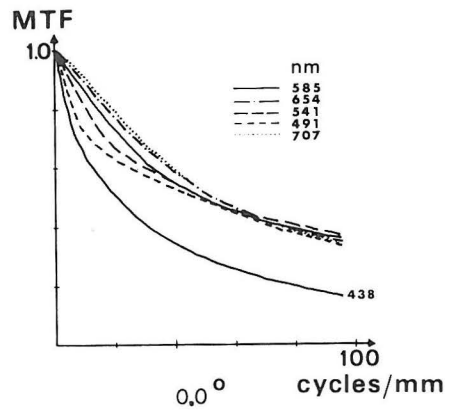


Fig. 20. MTF's with different wave lengths on the plane of best definition.

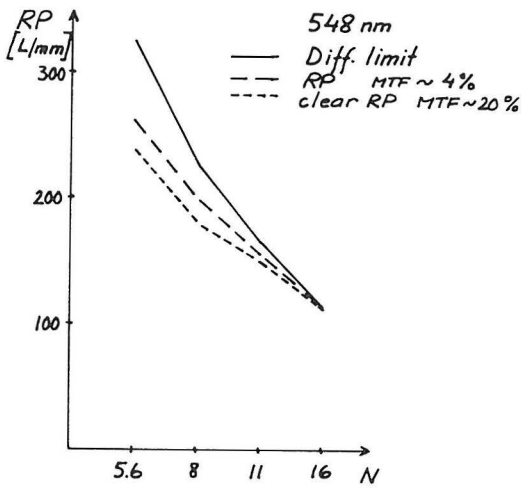


Fig. 11. RP on the axis with different apertures.

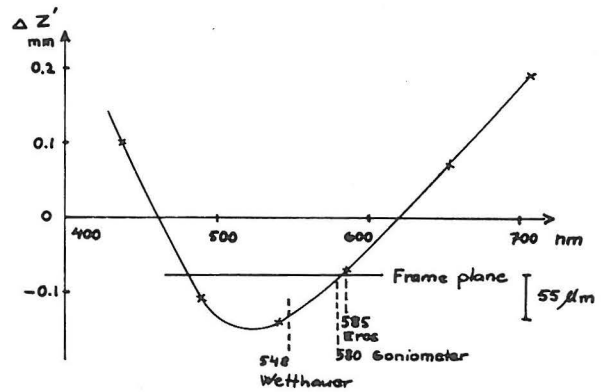


Fig. 13. Plane of best definition with different wave lengths.

cycles/mm	0.0°		14.6°		27.5°		33.1°		37.6°		40.7°		42.6°	
	T	R	T	R	T	R	T	R	T	R	T	R	T	R
10	1		4	0	12	15	7	20	9	10	0	2	-4	-6
20	2		4	4	12	15	-2	17	15	10	11	2	6	-3
30	3		4	9	1	8	-3	13	10	10	7	5	1	7
40	4		4	7	7	-3	3	9	7		4	1	1	-6
50	4		2	5	7			7	5		2			0
60	3		2	4	6			5						
70	0		1	1	5			3						
80	-1		-1	0	6			2						
90	-3		-2		5			1						

Table 1. Differences Helsinki-Braunschweig in the MTF measurement in %.